

First Study for the Pentaquark Potential in SU(3) Lattice QCD

Fumiko Okiharu

Department of Physics, Nihon University, 1-8 Kanda-Surugadai, Chiyoda, Tokyo 101, Japan

Hideo Suganuma

Faculty of Science, Tokyo Institute of Technology, 2-12-1 Ohokayama, Tokyo 152-8551, Japan

Toru T. Takahashi

Yukawa Institute for Theoretical Physics, Kyoto University, Kitashirakawa, Sakyo, Kyoto 606-8502, Japan

(Dated: November 1, 2018)

The static penta-quark (5Q) potential V_{5Q} is studied in SU(3) lattice QCD with $16^3 \times 32$ and $\beta=6.0$ at the quenched level. From the 5Q Wilson loop, V_{5Q} is calculated in a gauge-invariant manner, with the smearing method to enhance the ground-state component. V_{5Q} is well described by the OGE plus multi-Y Ansatz: a sum of the OGE Coulomb term and the multi-Y-type linear term proportional to the minimal total length of the flux-tube linking the five quarks. Comparing with QQ and 3Q potentials, we find a universality of the string tension, $\sigma_{Q\bar{Q}} \simeq \sigma_{3Q} \simeq \sigma_{5Q}$, and the OGE result for Coulomb coefficients.

The inter-quark force is one of the elementary quantities for the study of the multi-quark system in the quark model. As for baryons, our group recently studied the three-quark (3Q) potential V_{3Q} in detail with lattice QCD, and clarified that it obeys the Coulomb plus Y-type linear potential[1]. However, no one knows the inter-quark force from QCD in the exotic multi-quark system such as tetra-quark mesons (QQ- $\bar{Q}\bar{Q}$), penta-quark baryons (4Q- \bar{Q}), dibaryons (6Q) and so on.

Very recently, an exotic anti-strange baryon $\Theta^+(1540)$ with $S = +1$ was experimentally discovered at SPring-8 (LEPS), and was confirmed by ITEP(DIANA), JLab(CLAS) and ELSA(SAPHIR)[2]. The $\Theta^+(1540)$ was theoretically predicted in the Skyrme model[3], and is regarded as a penta-quark (5Q) baryon of $u^2d^2\bar{s}$ in the valence-quark picture. Another 5Q baryon $\Xi^{--}(1862)$ was found by CERN(NA49)[4], and also an anti-charmed 5Q baryon $\Theta_c(3099)$ was found by HERA(H1)[5].

Accordingly, many theoretical studies[6] have been done for the 5Q baryon using various approaches such as lattice QCD[7, 8], the constituent quark model[9], the diquark model[10], the QCD sum rule[11], the flux-tube model[12], the string theory[13] and so on. However, there are several puzzling problems on the $\Theta^+(1540)$: its mass seems to be rather small and its decay width is extremely narrow[2]. To solve them, one encounters the many-body problem of quarks, and therefore it is quite desired to clarify the inter-quark force in the multi-quark system based on QCD.

In this paper, motivated by the recent discovery of the penta-quark baryons, we perform the first study of the static penta-quark (5Q) potential V_{5Q} , i.e., the inter-quark force in the 5Q system, in SU(3) lattice QCD with $\beta=6.0$ and $16^3 \times 32$ at the quenched level. Note that the lattice QCD result of V_{5Q} presents a key information in modeling the multi-quark system based on QCD.

For the penta-quark system, we investigate the QQ- \bar{Q} -

QQ type configuration with the two ‘‘QQ clusters’’ belonging to the $\mathbf{3}^*$ representation of the SU(3) color as shown in Fig.1, since this type of the 5Q configuration is expected to have a small energy and seems to be natural as a realistic candidate of the $\Theta^+(1540)$. Indeed, in the perturbative sense, an attractive (repulsive) force acts between two quarks, when their total SU(3) color belongs to $\mathbf{3}^*$ ($\mathbf{6}$). Therefore, the nearest QQ cluster tends to form $\mathbf{3}^*$ rather than $\mathbf{6}$ in the low-lying 5Q system, which leads to the $\mathbf{3}^*$ -diquark model[10].

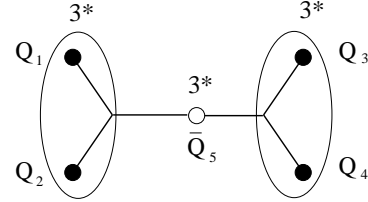


FIG. 1: The QQ- \bar{Q} -QQ type configuration for the penta-quark system. The two QQ clusters belong to the $\mathbf{3}^*$ representation of the color SU(3).

Similar to the derivation of the Q- \bar{Q} (3Q) potential from the (3Q) Wilson loop, the 5Q static potential V_{5Q} can be calculated with the 5Q Wilson loop W_{5Q} , which is defined in a gauge-invariant manner as shown in Fig.2.

We define the 5Q Wilson loop W_{5Q} [8] as

$$W_{5Q} \equiv \frac{1}{3!} \epsilon^{abc} \epsilon^{a'b'c'} M^{aa'} (\tilde{L}_3 \tilde{L}_{12} \tilde{L}_4)^{bb'} (\tilde{R}_3 \tilde{R}_{12} \tilde{R}_4)^{cc'}, \quad (1)$$

where \tilde{M} , \tilde{L}_i , \tilde{R}_i ($i = 1, 2, 3, 4$) are given by

$$\tilde{M}, \tilde{L}_i, \tilde{R}_i \equiv P \exp \left\{ ig \int_{M, L_i, R_i} dx^\mu A_\mu(x) \right\} \in \text{SU}(3)_c. \quad (2)$$

As shown in Fig.2, \tilde{M} , \tilde{L}_i , \tilde{R}_i ($i = 3, 4$) are line-like variables and \tilde{L}_i , \tilde{R}_i ($i = 1, 2$) are staple-like variables. Here,

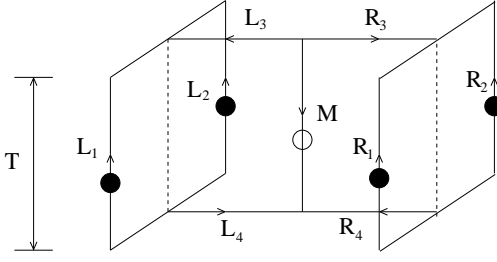


FIG. 2: The penta-quark (5Q) Wilson loop W_{5Q} for the 5Q potential V_{5Q} . The contours $M, L_i, R_i (i = 3, 4)$ are line-like and $L_i, R_i (i = 1, 2)$ are staple-like. The 5Q gauge-invariant state is generated at $t = 0$ and is annihilated at $t = T$ with the five quarks ($4Q\bar{Q}$) being spatially fixed in \mathbf{R}^3 for $0 < t < T$.

$\tilde{L}_{12}, \tilde{R}_{12} \in SU(3)_c$ are defined as

$$\tilde{L}_{12}^{a'a} \equiv \frac{1}{2} \epsilon^{abc} \epsilon^{a'b'c'} \tilde{L}_1^{bb'} \tilde{L}_2^{cc'}, \quad \tilde{R}_{12}^{a'a} \equiv \frac{1}{2} \epsilon^{abc} \epsilon^{a'b'c'} \tilde{R}_1^{bb'} \tilde{R}_2^{cc'} . \quad (3)$$

Note that the 5Q Wilson loop W_{5Q} is gauge invariant, and its gauge invariance is owing to the nontrivial assignment of the color indices of \tilde{L}_{12} and \tilde{R}_{12} in Eq.(3). (Recall that the “two quark lines” combining into the 3^* representation correspond to an “antiquark line” as the color current.)

In principle, the ground-state 5Q potential V_{5Q} is obtained from the 5Q Wilson loop $\langle W_{5Q} \rangle$ as $V_{5Q} = -\lim_{T \rightarrow \infty} \frac{1}{T} \ln \langle W_{5Q} \rangle$. However, the practical lattice calculation is done with a finite region of T , where excited-state contributions remain. For the accurate measurement of V_{5Q} in lattice QCD, we use the gauge-covariant smearing method[1] to enhance the ground-state component of the 5Q state in the 5Q Wilson loop.

The smearing is known to be a powerful method for the accurate measurement of the $Q\bar{Q}$ and the $3Q$ potentials[1], and is expressed as the iterative replacement of the spatial link variables $U_i(s)$ ($i=1,2,3$) by the obscured link variables $\bar{U}_i(s) \in SU(3)_c$ which maximizes $\text{Re tr} \{ \bar{U}_i^\dagger(s) V_i(s) \}$ with

$$V_i(s) \equiv \alpha U_i(s) + \sum_{\hat{j} \neq i} \sum_{\pm} \{ U_{\pm j}(s) U_i(s \pm \hat{j}) U_{\pm j}^\dagger(s + \hat{i}) \} \quad (4)$$

with the simplified notation of $U_{-j} \equiv U_j^\dagger(s - \hat{j})$. We here adopt $\alpha = 2.3$ and the iteration number $N_{\text{smr}} = 40$, which lead to a large enhancement of the ground-state component in the 5Q Wilson loop at $\beta=6.0$.

Now, we proceed the actual lattice QCD calculation for the 5Q potential V_{5Q} [8]. We generate 150 gauge configurations using $SU(3)_c$ lattice QCD with the standard action with $\beta = 6.0$ and $16^3 \times 32$ at the quenched level. The gauge configurations are taken every 500 sweeps after a thermalization of 5000 sweeps using the pseudo-heat-bath algorithm. The lattice spacing a is estimated as $a \simeq 0.104\text{fm}$ from the string tension $\sigma=0.89 \text{ GeV/fm}$ in the $Q\bar{Q}$ potential $V_{Q\bar{Q}}$ [8].

As for the 5Q configuration, we consider the $QQ\bar{Q}\bar{Q}$ type configuration as shown in Fig.1. Note that the multi-quark system including four or more quarks can take a three-dimensional shape, while the $Q\bar{Q}$ and the $3Q$ systems can take only planar configuration[8, 12]. Then, we investigate both the planar 5Q configuration as shown in Fig.3 and the twisted 5Q configuration as shown in Fig.4. In this paper, we take $d_1 = d_2 = d_3 = d_4 \equiv d$, and present the lattice QCD result of V_{5Q} in terms of (d, h_1, h_2) .

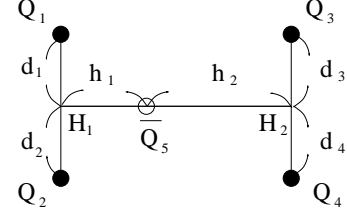


FIG. 3: A planar configuration of the penta-quark system. Q_1Q_2 is parallel to Q_3Q_4 , and H_1H_2 is perpendicular to Q_1Q_2 and Q_3Q_4 . Here, we take $d_1 = d_2 = d_3 = d_4 \equiv d$.

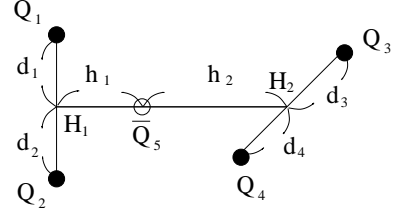


FIG. 4: A twisted configuration of the penta-quark system. Q_1Q_2 is perpendicular to Q_3Q_4 , and H_1H_2 is perpendicular to Q_1Q_2 and Q_3Q_4 . Here, we take $d_1 = d_2 = d_3 = d_4 \equiv d$.

For these types of 5Q configurations, we calculate the 5Q potential V_{5Q} from the 5Q Wilson loop $\langle W_{5Q} \rangle$ using the smearing method. Owing to the smearing, the ground-state component is largely enhanced, and therefore the 5Q Wilson loop $\langle W_{5Q} \rangle$ composed with the smeared link variable exhibits a single-exponential behavior as $\langle W_{5Q} \rangle \simeq e^{-V_{5Q}T}$ even for a small value of T . Then, for each 5Q configuration, we extract V_{5Q} from the least squares fit with the single-exponential form

$$\langle W_{5Q} \rangle = \bar{C} e^{-V_{5Q}T} \quad (5)$$

in the range of $T_{\text{min}} \leq T \leq T_{\text{max}}$ listed in Table I. The prefactor \bar{C} physically means the ground-state overlap, and $\bar{C} \simeq 1$ corresponds to the quasi-ground-state. Here, we choose the fit range of T such that the stability of the “effective mass” $V(T) \equiv \ln \{ \langle W_{5Q}(T) \rangle / \langle W_{5Q}(T+1) \rangle \}$ is observed in the range of $T_{\text{min}} \leq T \leq T_{\text{max}} - 1$. For the lattice calculation of $\langle W_{5Q} \rangle$, we use the translational and the rotational symmetries on lattices.

For 56 different patterns of the 5Q configurations as shown in Figs.3 and 4, we present the lattice QCD data for the 5Q potential V_{5Q} together with the ground-state

TABLE I: Lattice QCD results for the penta-quark potential V_{5Q} for the planar 5Q configuration labeled by (d, h_1, h_2) as shown in Fig.3. We list also the ground-state overlap \bar{C} , the fit range of T and the theoretical form V_{5Q}^{theor} of the OGE plus multi-Y Ansatz (8) with (A_{5Q}, σ_{5Q}) fixed to be (A_{3Q}, σ_{3Q}) in V_{3Q} in Ref.[1]. All the data are measured in the lattice unit.

(d, h_1, h_2)	V_{5Q}	\bar{C}	$T_{\min}-T_{\max}$	V_{5Q}^{theor}
(1,1,1)	1.4452(11)	0.9539(21)	2-7	1.4433
(1,1,2)	1.5409(13)	0.9506(25)	2-8	1.5414
(1,1,3)	1.6177(19)	0.9512(33)	2-7	1.6146
(1,1,4)	1.6793(20)	0.9431(35)	2-7	1.6767
(1,1,5)	1.7381(23)	0.9394(40)	2-6	1.7332
(1,1,6)	1.7918(28)	0.9311(49)	2-6	1.7866
(1,1,7)	1.8441(31)	0.9232(56)	2-6	1.8380
(1,2,2)	1.6314(17)	0.9503(29)	2-6	1.6322
(1,2,3)	1.7011(20)	0.9427(34)	2-5	1.7021
(1,2,4)	1.7680(25)	0.9478(43)	2-6	1.7623
(1,2,5)	1.8190(29)	0.9297(50)	2-6	1.8177
(1,2,6)	1.8717(33)	0.9205(57)	2-5	1.8704
(1,3,3)	1.7723(24)	0.9405(39)	2-4	1.7702
(1,3,4)	1.8336(28)	0.9351(49)	2-7	1.8293
(1,3,5)	1.8913(33)	0.9320(62)	2-5	1.8839
(1,4,4)	1.8939(31)	0.9293(53)	2-4	1.8877
(2,1,1)	1.7531(23)	0.9393(40)	2-5	1.7515
(2,2,2)	1.8803(31)	0.9292(54)	2-6	1.8887
(2,3,3)	2.0030(37)	0.9284(64)	2-5	2.0098
(2,4,4)	2.1122(49)	0.9116(91)	2-5	2.1211
(3,1,1)	1.9734(37)	0.9138(66)	2-5	1.9850
(3,2,2)	2.0811(45)	0.9070(75)	2-5	2.0942
(3,3,3)	2.1886(53)	0.9003(92)	2-4	2.2047
(3,4,4)	2.3043(68)	0.9084(113)	2-5	2.3105
(4,1,1)	2.1697(60)	0.8948(100)	2-5	2.1958
(4,2,2)	2.2734(60)	0.8890(100)	2-5	2.2829
(4,3,3)	2.3657(73)	0.8606(120)	2-4	2.3864
(4,4,4)	2.4706(104)	0.8534(164)	2-5	2.4884

overlap \bar{C} in Table I and II. The statistical errors are estimated with the jackknife method. We find a large ground-state overlap as $\bar{C} > 0.85$ for almost all 5Q configurations.

Next, we consider the theoretical form of the 5Q potential V_{5Q} . The lattice QCD studies[1] at the quenched level show that the Q- \bar{Q} potential $V_{Q\bar{Q}}$ takes a form of

$$V_{Q\bar{Q}}(r) = -\frac{A_{Q\bar{Q}}}{r} + \sigma_{Q\bar{Q}}r + C_{Q\bar{Q}}, \quad (6)$$

and the 3Q potential V_{3Q} takes a form of

$$V_{3Q} = -A_{3Q} \sum_{i<j} \frac{1}{|\mathbf{r}_i - \mathbf{r}_j|} + \sigma_{3Q}L_{\min} + C_{3Q}, \quad (7)$$

where L_{\min} denotes the minimal value of total length of color flux tubes linking the three quarks. In fact, both

TABLE II: Lattice QCD results for the penta-quark potential V_{5Q} for the twisted 5Q configuration labeled by (d, h_1, h_2) as shown in Fig.4. The notations are the same in Table I.

(d, h_1, h_2)	V_{5Q}	\bar{C}	$T_{\min}-T_{\max}$	V_{5Q}^{theor}
(1,1,1)	1.4476(23)	0.9378(64)	3-8	1.4458
(1,1,2)	1.5438(14)	0.9528(25)	2-8	1.5419
(1,1,3)	1.6155(17)	0.9459(31)	2-6	1.6148
(1,1,4)	1.6767(21)	0.9370(37)	2-6	1.6767
(1,1,5)	1.7365(22)	0.9357(42)	2-5	1.7332
(1,1,6)	1.7912(26)	0.9297(42)	2-4	1.7866
(1,1,7)	1.8337(88)	0.8933(231)	3-5	1.8380
(1,2,2)	1.6302(16)	0.9472(29)	2-8	1.6324
(1,2,3)	1.7022(18)	0.9445(32)	2-4	1.7022
(1,2,4)	1.7657(25)	0.9427(44)	2-5	1.7624
(1,2,5)	1.8232(30)	0.9385(51)	2-7	1.8177
(1,2,6)	1.8728(32)	0.9230(58)	2-8	1.8704
(1,3,3)	1.7710(24)	0.9376(42)	2-6	1.7702
(1,3,4)	1.8326(27)	0.9335(46)	2-4	1.8293
(1,3,5)	1.8952(32)	0.9394(58)	2-7	1.8839
(1,4,4)	1.8950(30)	0.9315(52)	2-4	1.8877
(2,1,1)	1.7735(23)	0.9377(41)	2-6	1.7615
(2,2,2)	1.8832(30)	0.9279(54)	2-7	1.8899
(2,3,3)	2.0011(37)	0.9233(64)	2-5	2.0100
(2,4,4)	2.1155(49)	0.9167(85)	2-6	2.1212
(3,1,1)	2.0049(37)	0.9032(67)	2-5	2.0008
(3,2,2)	2.0873(38)	0.8987(69)	2-4	2.0973
(3,3,3)	2.1870(54)	0.8912(92)	2-6	2.2055
(3,4,4)	2.3021(68)	0.9019(113)	2-5	2.3108
(4,1,1)	2.2141(65)	0.8741(107)	2-6	2.2155
(4,2,2)	2.2874(64)	0.8768(107)	2-5	2.2879
(4,3,3)	2.3715(70)	0.8577(118)	2-4	2.3880
(4,4,4)	2.4680(94)	0.8459(149)	2-4	2.4890

$V_{Q\bar{Q}}$ and V_{3Q} are described by a sum of the short-distance one-gluon-exchange (OGE) result and the long-distance flux-tube result[1, 14].

For the static penta-quark (5Q) system, we find that the lattice QCD results are well described by the OGE plus multi-Y Ansatz: a sum of the OGE Coulomb term and the multi-Y type linear term [8],

$$\begin{aligned} V_{5Q} &= \frac{g^2}{4\pi} \sum_{i<j} \frac{T_i^a T_j^a}{|\mathbf{r}_i - \mathbf{r}_j|} + \sigma_{5Q}L_{\min} + C_{5Q} \\ &= -A_{5Q} \left\{ \left(\frac{1}{r_{12}} + \frac{1}{r_{34}} \right) + \frac{1}{2} \left(\frac{1}{r_{15}} + \frac{1}{r_{25}} + \frac{1}{r_{35}} + \frac{1}{r_{45}} \right) \right. \\ &\quad \left. + \frac{1}{4} \left(\frac{1}{r_{13}} + \frac{1}{r_{14}} + \frac{1}{r_{23}} + \frac{1}{r_{24}} \right) \right\} + \sigma_{5Q}L_{\min} + C_{5Q} \quad (8) \end{aligned}$$

with $r_{ij} \equiv |\mathbf{r}_i - \mathbf{r}_j|$ and i th quark location \mathbf{r}_i in Fig.1. Here, L_{\min} is the minimal length of the flux-tube linking five quarks as shown in Fig.1. (For the extreme case, e.g., $d > \sqrt{3}h_1$, we here assume that the flux-tube is formed

as the two straight lines on Q_1Q_5 and Q_2Q_5 , considering the color combination, although there may appear several possibilities as the “flip-flop”.)

Note that there appear three kinds of Coulomb coefficients (A_{5Q} , $\frac{1}{2}A_{5Q}$, $\frac{1}{4}A_{5Q}$) in the penta-quark system, while only one Coulomb coefficient, $A_{Q\bar{Q}}$ or A_{3Q} , appears in the $Q\bar{Q}$ or the $3Q$ system. Here, the Coulomb coefficient A_{5Q} in Eq.(8) corresponds to A_{3Q} or $\frac{1}{2}A_{Q\bar{Q}}$ in terms of the OGE result.

We add in Table I and II the theoretical form V_{5Q}^{theor} of the OGE plus multi-Y Ansatz (8) with (A_{5Q}, σ_{5Q}) fixed to be (A_{3Q}, σ_{3Q}) in the $3Q$ potential V_{3Q} obtained in Ref.[1], i.e., $A_{5Q} = A_{3Q} \simeq 0.1366$, $\sigma_{5Q} = \sigma_{3Q} \simeq 0.046a^{-2}$ and $C_{5Q} \simeq 1.58a^{-1}$. (Note that there is no adjustable parameter for the theoretical form V_{5Q}^{theor} besides an irrelevant constant C_{5Q} , since A_{5Q} and σ_{5Q} are fixed to be A_{3Q} and σ_{3Q} , respectively.) Thus, the $5Q$ potential V_{5Q} is found to be well described by the OGE Coulomb plus multi-Y-type linear potential.

We show in Fig.5 typical examples of the lattice QCD data for the penta-quark potential V_{5Q} . The symbols denote the lattice data, and the curves denote the theoretical form of the OGE plus multi-Y Ansatz with (A_{5Q}, σ_{5Q}) fixed to be (A_{3Q}, σ_{3Q}) . One finds a good agreement between the lattice QCD data and the theoretical curves.

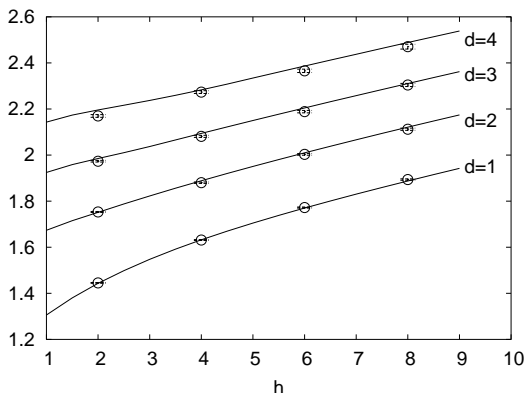


FIG. 5: Lattice QCD results of the penta-quark potential V_{5Q} for the planar $5Q$ configuration with $h_1 = h_2 \equiv h$ in Fig.3 in the lattice unit. Each $5Q$ system is labeled by d and h . The symbols denote the lattice data, and the curves the theoretical form of the OGE plus multi-Y Ansatz.

Note that the planar and the twisted $5Q$ configurations with the same (d, h_1, h_2) are almost degenerate, although the energy of the planar one is slightly smaller. In terms of the OGE plus multi-Y Ansatz, the only energy difference between the two states originates from a small difference of the Coulomb interaction between $Q_i (i = 1, 2)$ and $Q_j (j = 3, 4)$, where the Coulomb coefficient is reduced as $\frac{1}{4}A_{5Q} (\simeq \frac{1}{8}A_{Q\bar{Q}})$. Then, no special configuration is favored in the $5Q$ system in terms of the energy. This fact also indicates that the $5Q$ system is unstable against the twisted motion of the two $Q\bar{Q}$ clusters

as shown in Fig.4. In fact, general $5Q$ systems tend to take a three-dimensional configuration [8, 12] in terms of the entropy.

From the comparison with the $Q\bar{Q}$ and the $3Q$ potentials, the universality of the string tension and the OGE result are found among $Q\bar{Q}$, $3Q$ and $5Q$ systems as

$$\sigma_{Q\bar{Q}} \simeq \sigma_{3Q} \simeq \sigma_{5Q}, \quad \frac{1}{2}A_{Q\bar{Q}} \simeq A_{3Q} \simeq A_{5Q}. \quad (9)$$

This result supports the flux-tube picture on the confinement mechanism even for the multi-quark system [8].

To conclude, we have performed the first study of the penta-quark potential in lattice QCD, and have found that the $5Q$ potential is well reproduced by the OGE Coulomb plus multi-Y-type linear potential.

H.S. was supported in part by a Grant for Scientific Research (No.16540236) from the Ministry of Education, Culture, Science and Technology, Japan. T.T.T. was supported by the Japan Society for the Promotion of Science. The lattice QCD Monte Carlo calculations have been performed on NEC-SX5 at Osaka University.

-
- [1] T.T. Takahashi, H. Matsufuru, Y. Nemoto and H. Suganuma, Phys. Rev. Lett. **86**, 18 (2001); T.T. Takahashi, H. Suganuma, Y. Nemoto and H. Matsufuru, Phys. Rev. **D65**, 114509 (2002); T.T. Takahashi and H. Suganuma, Phys. Rev. Lett. **90**, 182001 (2003).
 - [2] LEPS Collaboration (T. Nakano *et al.*), Phys. Rev. Lett. **91**, 012002 (2003); DIANA Collaboration (V.V. Barmin *et al.*), Phys. Atom. Nucl. **66**, 1715 (2003); CLAS Collaboration (S. Stepanyan *et al.*), Phys. Rev. Lett. **91**, 252001 (2003); SAPHIR Collaboration (J. Barth *et al.*), Phys. Lett. **B572**, 127 (2003).
 - [3] D. Diakonov, V. Petrov and M. Polyakov, Z. Phys. **A359**, 305 (1997).
 - [4] NA49 Collaboration (C. Alt *et al.*), Phys. Rev. Lett. **92**, 042003 (2004).
 - [5] H1 Collaboration (A. Aktas *et al.*), hep-ex/0403017.
 - [6] For a recent review article, M. Oka, hep-ph/0406211, Prog. Theor. Phys. (2004), and references therein.
 - [7] F. Csikor, Z. Fodor, S.D. Katz and T.G. Kovacs, JHEP **11**,070 (2003); S. Sasaki, hep-lat/0310014 (2003).
 - [8] H. Suganuma, T.T. Takahashi, F. Okiharu, H. Ichie, Proc. of *QCD Down Under*, March 2004, Adelaide, to appear in Nucl. Phys. **B** (Proc. Suppl.) (2004).
 - [9] M. Karliner and H.J. Lipkin, hep-ph/0307243 (2003).
 - [10] R.L. Jaffe and F. Wilczek, Phys. Rev. Lett. **91**, 232003 (2003).
 - [11] S.-L. Zhu, Phys. Rev. Lett. **91**, 232002 (2003); J. Sugiyama, T. Doi and M. Oka, Phys. Lett. **B581**, 167 (2004).
 - [12] X.-C. Song and S.-L. Zhu, hep-ph/0403093.
 - [13] I.M. Narodetskii, Yu.A. Simonov, M.A. Trusov and A.I. Veselov, Phys. Lett. **B578**, 318 (2004); M. Bando, T. Kugo, A. Sugamoto, S. Terunuma, hep-ph/0405259.
 - [14] H. Ichie, V. Bornyakov, T. Streuer and G. Schierholz, Nucl. Phys. **A721**, 899 (2003); Nucl. Phys. **B** (Proc. Suppl.) **119**, 751 (2003).